

Dear authors,

Thanks for incorporating my comments and suggestions from the first round. The manuscript has already been improved. However, there is still some work to do in my opinion. I commented the manuscript with suggestions and questions. Main points are:

Still not clear how you classify fringe patterns. Many areas which look very similar are classified differently in different regions. See my comments in the manuscript to the Laptev Sea, for example. Therefore, I suggest to describe the manual procedure and add representative examples in Methods, as well as in the Results.

Structure of the paper can be improved. The entire chapter on the ice arch can be split and parts could be moved to the Introduction, Methods, Results and Discussion accordingly. The chapter on the comparison of your results with previous studies should be a part of Discussion. Your very results could be presented in a more detailed way, again with examples.

Furthermore, I insist on a professional proofreading to make the writing clearer and smoother. Many sentences could be simplified and shortened.

I hope to see the updated version of your manuscript soon!

Best regards,

Your reviewer

~~Landfast sea ice stability mapping pan-Arctic ice regimes with implications for ice use, subsea permafrost and marine habitats~~

Dyre O. Dammann¹, Leif E.B. Eriksson¹, Andrew R. Mahoney², Hajo Eicken³, Franz J. Meyer²

¹Department of Earth, Space, and Environment, Chalmers University of Technology, Gothenburg, 412 96, Sweden

5 ²Geophysical institute, University of Alaska Fairbanks, Fairbanks, 99775, USA

³International Arctic Research Center, University of Alaska Fairbanks, Fairbanks, 99775, USA

Correspondence to: Dyre O. Dammann (dyre.dammann@chalmers.se)

Abstract. Arctic landfast sea ice has undergone substantial changes in recent decades affecting ice stability with potential impacts on ice travel by coastal populations and industry ice roads. The role of landfast ice as an important habitat has also evolved. We present a novel approach to evaluate sea ice stability on a pan-Arctic scale using Synthetic Aperture Radar Interferometry (InSAR). Using Sentinel-1 images from spring 2017, the approach discriminates between bottomfast, ~~with critical relevance for subsea permafrost, as well as~~ stabilized and non-stabilized floating landfast ice over the main marginal seas of the Arctic Ocean (Beaufort, Chukchi, East Siberian, Laptev and Kara Seas). The analysis draws on evaluation of ~~small-scale lateral motion derived from~~ relative changes in interferometric fringe patterns. This first comprehensive assessment of Arctic bottomfast sea ice extent revealed that by area most of the bottomfast sea ice is situated around river mouths and coastal shallows in the Laptev and East Siberian Seas, covering roughly 4.1 and 5.1 thousand km² respectively. The fraction between non-stabilized and stabilized ice is lowest in the Beaufort at almost unity, and highest in the adjacent Chukchi Sea. Beyond the simple mapping of landfast ice zones, this work provides a new understanding of how stability zones may vary between regions and over time. InSAR-derived stability data may serve as a strategic planning and tactical decision-support tool for different uses of coastal ice. Such information may also inform assessments of important sea ice habitats. In a case study, we examined an ice arch situated in Nares Strait demonstrating that interferograms may reveal early-warning signals for the break-up of stationary sea ice.

1 Introduction

1.1 Landfast sea ice stability and stakeholder dependence

25 Sea ice is an important component of Arctic ecosystems and provides important services as a climate regulator (Screen and Simmonds, 2010), habitat for marine biota (Thomas, 2017), as well as a platform for coastal populations (Krupnik et al., 2010). During the last century, an expansion of transportation and resource extraction have led to increased human presence in the Arctic and further diversification of ice use (Eicken et al., 2009). The recent retreat of sea ice observed throughout the past several decades (Stroeve et al., 2012; Comiso and Hall, 2014; Meier et al., 2014) has already resulted in widespread consequences for ice users (Druckenmiller et al., 2013; Aporta and Higgs, 2005; Fienup-Riordan and Rearden, 2010; Orviku et al., 2011; ACIA, 2004) and increasing hazards (Eicken and Mahoney, 2015; Ford et al., 2008). At the same time, the related increased accessibility to Arctic waters (Stephenson et al., 2011) is leading to increasing ship traffic and resource exploration (Lovecraft and Eicken, 2011; Eguiluz et al., 2016). It is recognized that the sea ice conditions for future Arctic marine operations will be challenging and will require substantial monitoring and improved regional observations (Ellis and Brigham, 2009) at the scale necessary for assessing environmental hazards and effective emergency response (Eicken et al., 2011).

Most of the Arctic ocean is dominated by drifting pack ice, whereas stationary landfast ice occupies much of the Arctic coastlines roughly between November and June depending on location (Figure 1) (Yu et al., 2014). Although the landfast ice is stationary, it does deform internally at the cm- to m-scale on timescales of days to months (Dammann et al., 2016). The often several km to up to hundreds of km wide sections of landfast ice are held in place by grounded ridges, islands, or coastline morphology, such as embayments or fjords. Similar to the drifting pack ice, landfast ice has declined significantly during the last few decades, in particular in terms of delayed freeze up (Mahoney et al., 2014; Selyuzhenok et al., 2015). Later freeze up critically impacts stakeholders through increased mobility (reduced stability) of the landfast ice in response to wind, ocean, or ice forcing (Dammann, 2017). Previous research suggests that landfast ice stability can be expressed in terms of the combined frictional resistance provided by relevant grounding or attachment points (e.g., islands and grounded ridges) (Druckenmiller, 2011; Mahoney et al., 2007b). The stability in part determines the rate at which the ice deforms and ultimately the severity of break-out events or magnitude of structural defects. We therefore suggest that landfast sea ice can be further categorized into four regimes, defined through their respective stability (Table 1). A typical landfast ice regime is illustrated in Figure 2, where the stability of the landfast ice area decreases from the coast towards the open ocean (Dammann et al., 2016).

Bottomfast sea ice can grow laterally to the km-scale during winter depending on local bathymetry (Solomon et al., 2008; Stevens et al., 2010). The bottomfast ice allows for heat loss from the sea floor and is therefore an integral part of aggregating and maintaining subsea permafrost (Stevens et al., 2008; Stevens et al., 2010; Stevens, 2011), controlling coastal stability/morphology (Eicken et al., 2005; Are and Reimnitz, 2000), and sediment properties (Solomon et al., 2008). Bottomfast ice is also relevant for fish as it reduces habitable shallow waters during winter (Hirose et al., 2008). Bottomfast ice is also of importance for on-ice operations as it can support a much larger load than floating ice. High to moderately stable landfast ice is of relevance to industrial (Potter et al., 1981) and subsistence ice use (Druckenmiller et al., 2013), but also for habitats (Tibbles et al., In press). For instance, ringed seals are dependent on stable landfast ice for denning (Smith, 1980). Low-stability ice is potentially relevant for ocean-based operations such as shipping through trans-Arctic passages close to the coast where patches of landfast ice occasionally break off and drift into nearby shipping lanes, potentially causing hazards. Even areas hundreds of km from landfast ice can be impacted through the failure of ice arches. Ice arches consist of stationary ice forming between islands during freeze-up and when collapsing in the spring can send hazardous old ice into shipping routes (Bailey, 1957; Wilson et al., 2004; Barber et al., 2018). Stability is also of relevance for destination cargo shipping in the Arctic as less stable, thinner ice is easier to break through resulting in opportunities for docking in areas of substantial landfast ice. For navigating through landfast ice, stabilization through ridging is also important to identify since ridges can be problematic to navigate and are often associated with hazards (Hui et al., 2017).

30 1.2 Remote sensing of landfast ice stability

Satellite remote sensing is an important tool for measuring ice conditions in the Arctic, including mapping of landfast ice (Muckenhuber and Sandven, 2017). Optical/thermal satellite data such as from the Advanced Very High Resolution Radiometer (AVHRR) were used to produce operational ice charts until the early 1990s when SAR was introduced into the charting production (Yu et al., 2014) as a superior data set due its independence of light and weather conditions and due to its higher (~100 m) resolution, both advantageous to stakeholders (Eicken et al., 2011). Different information products exist to map the boundary of landfast sea ice, typically derived by evaluating unchanged sections of ice between consecutive SAR backscatter scenes (Johannessen et al., 2006; Mahoney et al., 2014; Giles et al., 2008). Beside its use in mapping of landfast ice, SAR backscatter also has the ability to help discriminate between multiyear and first-year ice (Onstott, 1992) and identify different roughness regimes

(Dammann et al., 2017). However, backscatter does not give information pertaining to ice stability since the internal movement of the landfast ice is too small (mm/day) to be identified with change detection.

SAR interferometry (InSAR) is a signal processing technique, which extracts the phase difference between two SAR images acquired from similar viewing geometries. This phase difference (typically referred to as interferometric phase) can either signify topography if acquisitions are separated in space (i.e., non-zero perpendicular baseline) or measures the line-of-sight motion of an

~~observed feature~~ if acquisitions are separated in time (non-zero temporal baseline) (Ferretti et al., 2007; Bamler and Hartl, 1998). InSAR has been used to successfully map landfast ice (Meyer et al., 2011) as well as to provide information pertaining to landfast ice dynamics (Marbouti et al., 2017; Li et al., 1996; Vincent et al., 2004; Morris et al., 1999) and topography (Dammann et al., 2017; Dierking et al., 2017). In recent studies, InSAR has also been shown to reveal plausible rheologies for landfast ice (Dammert et al., 1998) and has been used to determine the origin of internal ice stresses (Berg et al., 2015). Combined with inverse modeling, InSAR also allows to determine ice deformation modes (Dammann et al., 2016), rates, and the associated stress and fracture potentials (Dammann et al., 2018b).

These studies have demonstrated the potential of InSAR as a tool to assess landfast ice dynamics and stability through localized case studies. They also laid the foundation for applying InSAR on a larger scale, potentially as a mean to generate operational information products and evaluate long-term trends. The coverage and access to InSAR-compatible SAR scenes has been an obstacle in the past, but has improved significantly since the launch of Sentinel-1. The suitability of Sentinel-1 for automatic SAR processing was shown, e.g., in Meyer et al. (2015). Hence, we explore InSAR as a tool to provide pan-Arctic information pertaining to stability relevant to subsea permafrost, biological habitats, and sea ice use. The goal of this work is to determine the Sentinel-1 interferometric data availability along substantial parts of the circumpolar coastlines, and explore whether the different ice stability regimes can consistently be analyzed and mapped in different geographic regions. We further explore limitations of the technology and the utility for long-term assessments of change. We also evaluate the kind of sea ice information that can be extracted directly from InSAR with operational relevance in terms of tactical and strategic decision making, without costly or complex algorithms.

2 Data and methods

2.1 Satellite data and study area

This study utilizes Sentinel-1, a constellation of two C-band SAR systems (Sentinel-1A and B) operating since 2014 and 2016, respectively, with a repeat-pass interval of 6 to 12 days depending on if both satellites acquire data or only one of them. Owing to the free-and-open data policy and large spatial coverage, Sentinel-1 acquisitions were obtained for five marginal seas of the Arctic ocean including the Beaufort, Chukchi, East Siberian, Laptev, and Kara Seas, enabling mapping of landfast sea ice on a pan-Arctic scale. All images used were captured in interferometric wideswath (IW) mode with a single-look resolution of roughly 3 m x 22 m in slant range and azimuth respectively and a ~250 km swath width. Images were almost exclusively acquired between March and May 2017 (see supplementary data for full list of images used). The Beaufort Sea coast of Alaska was used for comparison, as the sea ice in this area includes all four landfast ice regimes (bottomfast ice, semi-enclosed lagoon ice, ice stabilized by grounded ridges and islands, and areas with floating extensions of ice; Table 1), and as ample validation data is available from previous landfast sea ice studies. Alaska's Beaufort Sea coast is also of major interest in the context of local and indigenous ice use as well as industry resource exploration and extraction.

2.2 InSAR-based detection of landfast ice

The interferometric phase may be related to the lateral (e.g., thermal contraction or displacement due to compressional or shear forces) or vertical (e.g., through buckling or tidal displacement) sea ice motion occurring in between the acquisition times of the two InSAR images. A phase signature can sometimes also be attributed to factors not related to surface motion or topography such as atmospheric phase delay and coregistration errors, but these effects are small compared to ice motion and can often be corrected (Scharroo and Visser, 1998). Depending on the perpendicular baseline, sea ice topography can have a modest impact on the phase difference. Due to the tight baseline limits (<50 m standard deviation) of the Sentinel-1 constellation and as sea ice topography rarely exceeds 10 m, impacts on the interferogram interpretation are minimal for the data shown here (Dammann et al., 2016). Of the phase change attributed to motion, only displacement in line-of-sight direction (Δr_{LOS}) results in a phase change $\Delta \Phi_{disp}$ according to $\Delta \Phi_{disp} = 4\pi \Delta r_{LOS} / \lambda$ and the observed phase is measured within the wrapped interval of $[0; 2\pi]$. For Sentinel-1, the sensor wavelength λ is 5.66 cm, such that ice lateral displacement has to exceed $\Delta r_{LOS} \approx 5\text{ cm}$ for the $\Delta \Phi_{disp}$ phase values to result in more than one fringe and ambiguous phase values. The interferogram is a series of fringes representing the projection of the true three-dimensional ice motion onto the line-of-sight vector. The orientation of the fringes can be used to interpret the direction of the three-dimensional motion field while the fringe spacing is an indicator of the deformation rate. The interpretation of observed fringe patterns is, however, not straightforward typically requiring the use of an inverse model (Dammann et al., 2016).

The interferometric phase values will only be useful if scattering elements remain largely unchanged throughout the time interval bracketed by the image pairs used in processing. Coherence (ranging between 0 and 1) is a measure of the quality of the interferogram, which in general is high if scatterers remain unchanged and low if there is significant change in the scattering medium (Meyer et al., 2011). For the 6 or 12-day repeat cycle supported by Sentinel-1, the coherence over landfast ice was found to be generally high due to its stationary nature. Significant decorrelation can however occur in late spring as the onset of melt at that time causes substantial changes in the scattering medium. In this work, we have obtained images as close to late April as possible. This time frame was found to be ideal for our purpose as ice thickness is near its maximum leading to maximum stability without risking impacts from the onset of melt. All interferograms in this work were produced using a standard Sentinel-1 workflow. The images were first geometrically coregistered to ensure that the images cover exactly the same area with sub-pixel accuracy. The images were then multi-looked by averaging 10 pixels in range and 2 pixels in azimuth, resulting in reduced speckle and a final pixel spacing of roughly 23x28 m. Next, spectral filtering was performed to ensure both images comprise the same spectral range, reducing phase noise in the final interferogram. The interferometric phase was calculated for each pixel of the coregistered and filtered images. Furthermore, the expected phase ramp in cross-track direction from a stationary flat earth surface was removed. The phase noise of the final interferogram was reduced using an adaptive phase filter (Goldstein and Werner, 1998). All of these steps were completed for each interferogram using the GAMMA RS software (Werner et al., 2000).

2.3 Mapping of landfast ice zones

In this work, we are looking at the fringe spacing to roughly determine relative ice stability. There are many factors that affect fringe density in addition to stability, including the atmospheric and ocean forcing conditions, satellite viewing geometry, and the prevalent mode of ice deformation (Dammann et al., 2016), making it problematic to evaluate absolute stability from fringe density alone. Instead, we focus on abrupt changes in fringe spacing within individual interferograms that allow us to identify variations within an area imaged under largely the same conditions. Trends from higher to lower fringe density will, in such cases, likely correspond to increasing ice stability. We hypothesize that fringe density can reveal three different stability zones: bottomfast ice, stabilized ice, and non-stabilized ice (Table 1). The often-strong fringe gradient leading to an area of near-zero phase change has

been shown to represent the boundary of where the ice is frozen to the sea floor and can subsequently be used to map bottomfast ice (Dammann et al., 2018c). In Table 1, the two sheltered regimes will both lead to reduced fringe density and can be difficult to discriminate based on InSAR data alone. These regimes are therefore assigned to the zone “stabilized ice”. The three zones (i.e. bottomfast ice, stabilized ice, non-stabilized ice) are subjectively and manually mapped without the use of specific threshold values. 5 The zones themselves are therefore based on relative stability in terms of whether the ice is anchored or sheltered. A measure of whether the ice is stable would depend on the specific stakeholders and their dependence on stability. As an example, on shorter time scales, industry ice roads would be able to accommodate less strain than community ice trails due to different mode of transportation and user specific needs. Further steps to identify such thresholds are outlined in Dammann et al. (2018a).

The approach we present here, opens up the possibility of mapping landfast sea ice zones on a pan-Arctic scale. To demonstrate, 10 we used Sentinel-1 data acquired March through May 2017 and generated 52 interferograms that cover almost the entire continental coastlines of the Beaufort, Chukchi, East Siberian, Laptev, and Kara Seas. To reduce computational costs, we omitted Greenland, some island groups and in particular the Canadian Archipelago, which are characterized by extensive coastline lengths. The Alaskan and Russian coastlines have high economic significance for the shipping and natural resource industries and feature dynamically diverse ice regimes and large areas of bottomfast ice are expected in these regions. Except for one approximately 50 15 km-long section of coast in the Kara Sea and the eastern Laptev Sea, multiple InSAR compatible pairs were available for the specified time frame. This allowed us to select interferograms centered around the end of April, when most Arctic landfast ice is at its maximum extent. Coherence loss was evident in some areas, in particular in the Chukchi Sea, such as in the Kotzebue Sound likely partly due to ice motion, subsurface thinning from river runoff, and low signal-to-noise ratio. However, to ensure a realistic representation of what an operationally-produced synoptic, contiguous pan-Arctic interferogram would look like, we did not 20 attempt to derive alternative interferograms in these cases.

3 Results

3.1 Mapping pan-Arctic ice stability zones

The interferograms produced in this work (Figure 3) allowed for a detailed map of landfast ice including the identification of three landfast ice stability zones: bottomfast ice, stabilized landfast ice, and non-stabilized landfast ice. To our knowledge, our results 25 (Figure 4) represent the first mapping of bottomfast ice extent at this scale and the first attempt at any scale to map the extents of different landfast ice stability zones. ~~Subject to the considerations included in the discussions, it is clear that~~ most areas with extensive bottomfast ice reaching several km from shore are located either in the vicinity of river deltas or within lagoons. However, a prominent exception is the coastline of the western East Siberian Sea, where our analysis shows substantial amounts of bottomfast ice even tens of kilometers away from any major rivers. The East Siberian Sea with its three large river systems (the Indigirka, Bogdashkina, and Kolyma Rivers) contains the most bottomfast ice of the regions considered here (Table 2). The Laptev Sea also 30 contains a large fraction of the Arctic bottomfast sea ice mostly concentrated around the Lena and Yana Deltas.

The map of “stabilized” and “non-stabilized” landfast ice is based on subjective interpretation of the interferograms. Both stabilized and non-stabilized landfast ice zones were found in all marginal seas (Table 2), though their relative contributions to overall landfast ice extent varied widely. For example, in the Chukchi Sea, we identified the vast majority of the landfast ice as non-stabilized, with stabilized landfast ice occupying less area than the bottomfast ice. Conversely, the greatest area of stabilized 35 landfast ice was found in the adjacent Beaufort Sea, with a larger extent of stabilized than non-stabilized landfast ice.

In the East Siberian, Laptev and Kara Seas, the distinction between stabilized and non-stabilized landfast ice is not as straightforward as in the Beaufort and Chukchi Seas. Even so, it is clear that landfast ice extent in the East Siberian, Laptev and Kara Seas is dominated by vast areas of non-stabilized ice. Unlike the Chukchi Sea, we still identified significant areas of stabilized landfast ice along the Russian Arctic coast. In the Kara Sea, these are primarily found between the islands of the Nordenskiöld Archipelago in the east, but the most extensive regions of stabilized landfast ice in our study region (those that extend furthest from the coast) are found in the Laptev and East Siberian Seas (areas labeled A, B, and C in Figure 4).

3.2 Comparing stability zones with areas of known ice stability

To investigate whether the stability zones are reasonable, we compare our delineations to two areas (i.e. the Laptev and Beaufort Seas) where the landfast sea ice has been tracked over several years resulting in information pertaining to landfast sea ice stability. Due to limited SAR data availability in the central part of the Laptev Sea, the interferogram of the ice surrounding the Stolbovoy Island had to be acquired as early as February before the time of maximum ice stability (Figure 3). Even so, it is clear that the area to the northwest of the island features stabilized ice (see “D” in Figure 4). The stabilized ice area appears triangular due to the much earlier acquisition date of the surrounding interferogram. This exact area features a shoal of < 10 m water depth leading to earlier formation of fast ice than the surrounding areas (Selyuzhenok et al., 2015) likely due to the formation of grounded ridges on the shoal resulting in increased stability. The ability of interferometry to identify stabilized ice in this region lends support to our approach.

We will also consider the landfast ice along the Alaska Beaufort Sea coastline, which has been extensively researched and tracked in terms of its annual cycle and decadal variability (Mahoney et al., 2007a; Mahoney et al., 2004). The resulting stack of all landfast ice edges for all months between 1996 and 2008 (Mahoney et al., 2014) is plotted in Figure 5a. From this figure, it is clear that in certain regions, the ice extent is similar over time scales from months to years (see areas highlighted in the figure). It was found that these regions (“nodes”) of consistent landfast ice extent are often tied to the location of the 20-m isobath, a water depth associated with grounding of pressure ridges (Mahoney et al., 2014) (Figure 5a). A field study and indigenous knowledge also indicate persistent grounded ridges in the location of the node closest to Utqiagvik, Alaska (Meyer et al., 2011).

We created three interferograms acquired during the period April 8 – May 9 to cover the same stretch of coastline. The respective master images exhibit a sharp discontinuity in backscatter (see arrows in Figure 5b) along the general location of the landfast ice edge from Figure 5a and can be assumed to be the landfast ice edge. Determining the landfast ice edge can in some instances be achieved by evaluating a single amplitude image as here, but is not consistent and only works in cases where there are stark discontinuities in backscatter due to different ice types or a severely deformed landfast ice edge. The interferograms indicate in this case a similar landfast ice edge by a complete loss of coherence seaward of the discontinuity apparent in Figure 5b (Figure 5c). These interferograms reveal a wide range of fringe densities, ranging from near constant phase for areas close to the coast to the point where fringes are dense enough to almost merge near the landfast ice edge. It is also apparent that the fringe density does not linearly increase with distance from the coast, but rather changes along two distinct discontinuities.

One discontinuity separates the area of near-zero phase change from an area with relatively low fringe density. This discontinuity indicates the boundary between bottomfast and floating ice as two of these interferograms were validated both on Elson Lagoon near Utqiagvik and the Colville Delta (Dammann et al., 2018c). The second discontinuity appears to largely coincide with locations of the nodes identified by Mahoney et al. [2007a; 2014], which are thought to be associated with reoccurring grounded ice features (Figure 5a) (Meyer et al., 2011). This finding is expected since grounded ridges are known to stabilize the landfast ice leading to reduced strain shoreward of the grounding points (Mahoney et al., 2007b; Druckenmiller, 2011).

The discontinuity is not a straight line, but features multiple curves towards land ending in seaward points. At these points, the stability is higher than adjacent areas with the same distance from shore similar to the expected increased stability directly shoreward of grounded ridges. We performed a subjective, manual mapping (i.e. without the use of a specific threshold) of the strong phase gradients in Figure 5d and concluded that the ice regions separated by these discontinuities consist of non-stabilized, stabilized, and bottomfast ice (Figure 5e). Although the landfast ice edge can in some instances be mapped using a single backscatter image, the mapping of bottomfast and stabilized ice cannot be discriminated as is apparent by comparing the map from Figure 5e with Figure 5b.

4 Discussion

4.1 Methodological limitations for mapping stability zones

10 Although there are a number of sources of uncertainty that affect our map of landfast ice and its relative stability, ~~it is clear that not all landfast ice is equally stable and at least three different zones of stability have been identified.~~ In some areas, ~~the map of bottomfast ice has had to be approximated on the sub-km scale~~ due to ambiguities associated with low fringe density or fringes parallel to the bottomfast ice edge (Dammann et al., 2018c). We also acknowledge that small islands or sandbars not represented by our coast mask may be erroneously identified as bottomfast ice. However, we greatly reduced such errors by not mapping areas that appears to be low-laying land and sediment bars in the SAR backscatter images. This can lead to the appearance of sporadic areas of bottomfast ice, separated by areas with a phase resembling that of bottomfast ice, but which in reality is land. In areas where the landmask (Wessel and Smith, 1996) does not appear to fit the coastline, mapping the intricate coastal morphology can be a time-consuming task, hence mapping on a pan-Arctic scale will inevitably contain inaccuracies. However, these uncertainties are unlikely to significantly affect our findings at regional and pan-Arctic scales.

20 In this work, we did not apply strict mapping thresholds to distinguish between stabilized and non-stabilized ice, but rather made subjective determinations based on fringe patterns. This approach works well in the Chukchi and Beaufort Seas, where regions of low fringe density lie adjacent to the coast or bottomfast ice and can be easily mapped from regions of higher fringe density. However, in some regions, especially in the Russian Arctic, there is often a lack of distinct boundaries between regions of different fringe spacing, introducing ambiguities between stabilized and non-stabilized ice on scales from km to even tens of km. The difficulty distinguishing these two zones ~~of landfast ice in the Russian Arctic~~ may result from a reduced level of dynamic pack ice interaction along the Russian shelf, given the predominately divergent ice regime (Reimnitz et al., 1994; Jones et al., 2016; Alexandrov et al., 2000). Such ice regime is expected to ~~feature reduced~~ dynamically-induced strain (and therefore fewer interferometric fringes) in landfast ice seaward of offshore islands and grounded ridges making the non-stabilized ice appear more stable. Additionally, the greater extent of landfast ice on the shoreward side of grounding points provides a greater fetch, which may cause stabilized ice on the Russian Shelf to exhibit higher fringe densities than in the Chukchi or Beaufort Seas. This suggests, that there is likely a spectrum of landfast ice stability and additional zones may be necessary to fully characterize the landfast ice regimes in different regions and for different ice uses or research aims.

One potential candidate for reclassification is landfast ice in sheltered bays such as the Khatanga Gulf in the western Laptev Sea, which exhibited high fringe densities (Figure 3) and was hence identified as non-stabilized despite being nearly landlocked (Figure 4). Due to the shallow water in this region, it is likely that the high fringe density is caused in part by vertical motion associated with tides and coastal set up. Since vertical motion has less impact on stability in well-confined landfast ice, such examples suggest the need for an additional zones of stability that allows higher fringe densities in coastally confined regions. Another, larger-scale

example is the eastern Laptev sea, which is an area of landfast ice sheltered by the New Siberian Islands and is typically considered highly stable (Eicken et al., 2005). However, based on relatively high fringe density, in particularly offshore of the Lena Delta, we classify landfast ice in this region as non-stabilized (Figure 4).

This suggests that landfast ice in this region may be less stable than previously thought and a “partially stabilized” zone may be appropriate. This would be consistent with a recent SAR backscatter analysis of landfast ice in the Laptev Sea (Selyuzhenok et al., 2017), which showed that areas identified as landfast ice in operational ice charts may actually contain pockets of partly mobile ice over one month after initial landfast ice formation. Based on the overall fringe counts and patterns, only part of the phase response is likely attributed to tidal motion. ~~The number of useful zones of landfast ice stability~~ is limited by other inherent sources of uncertainty including sensitivity to specific atmospheric and oceanographic conditions during the time period between SAR acquisitions. For example, in the absence of dynamic interaction with pack ice, there may be little difference in fringe spacing between landfast ice seaward and shoreward of stabilizing anchor points. Without evaluating the phase response for each area of interest in detail during different forcing scenarios, it may be problematic to understand under what conditions the ice remains stable. Classification of stability based on relative differences in fringe density is also complicated by the use of non-simultaneous interferograms to provide complete coverage of a region. The interferograms used here were obtained as close to maximum ice extent and stability as possible (roughly late April), but sometimes had to be obtained as early as early March. Fringe density tends to decrease over the winter as the ice thickens. Hence, the use of interferograms based on different dates can aid interpretation by confirming consistent fringe patterns and identify temporal changes. However, the temporal change will also result in a phase gradient at the image stitching not related to different stability zones, which may further complicate the mapping process.

The Sentinel-1 interferograms considered here has a minimum temporal baseline of 12 days. Even if this baseline is shorter than what has been used in the past (Dammann et al., 2016; Mahoney et al., 2004), it is unlikely that the mapping of the seaward landfast ice edge incorporates stationary pack ice (as could possibly be the case for a 6-day baseline). Some regions feature consistent coherence loss such as the Kotzebue Sound region. Such regions can most often be identified through a spatially gradual progression from high coherence to a complete loss of coherence, where an exact map of landfast ice type boundaries is not possible. It is worth mentioning that this technique can only be used before the onset of melt when widespread coherence loss occurs, hence it is not possible to evaluate the retreat of bottomfast ice or reduction of ice stability in response to melt. Furthermore, IW imagery are predominately acquired over land, hence it is likely not possible to construct interferograms away from the coast to cover extensive landfast ice approaching the 250 km IW swath such as that in the East Siberian Sea.

4.2 Temporarily stabilized pack ice

Prior studies have demonstrated the utility of InSAR over landfast ice as a planning tool for on-ice operations (Dammann et al., 2018a; Dammann et al., 2018b) but we argue here that such utility and potential applications also extend to maritime activities and shipping. In regards to the latter, vessel traffic typically does not traverse landfast ice. However, the assessment of landfast ice stability and spatio-temporal extent can aid management of conflicting ice uses such as in the case of the access route to the Voisey’s Bay mine in the Canadian Arctic which cuts through landfast ice that is part of a traditional Nunatsiavummiut use area (Bell et al., 2014). For vessel traffic through ice-covered straits or archipelagos, the approach outlined here can help identify and evaluate hazards associated with ice arches. Ice arches form when ice passing through a narrow passage experiences flow stoppage as a result of confining pressure and behaves like landfast ice, though potentially without cohesive strength between individual floes (Hibler et al., 2006). Ice arches typically form between November and March (Moore and McNeil, 2018) and can block export of ice through straits as wide as 100 km (Melling, 2002).

Indeed, ice arches may be considered as an additional zone of “temporarily stabilized pack ice”. When formed, such arches represent a significant obstacle to marine traffic due to the high confining pressures that make icebreaking impossible for all but the most powerful vessels. The arches can in some locations prevail into the following season (Melling, 2002), but typically collapse in July – August (Kwok, 2005). Conversely, their break-up can lead to advection of large amounts of thick multiyear ice into high-traffic shipping routes (Barber et al., 2018) which is a well-known hazard for shipping (Bailey, 1957; Howell et al., 2013). SAR data have previously been used to estimate the advection of ice through straits in the Canadian Archipelago (Kwok, 2006; Melling, 2002; Howell et al., 2013). One location of particular interest is the Nares Strait situated in between Greenland and Ellesmere Island (Figure 6a), which features a seasonal ice arch (Kwok et al., 2010; Kwok, 2005) with important implications on the multiyear ice budget of the Arctic Ocean (Kwok et al., 2010). Here, we go beyond the detection of the presence of ice arches and explore the potential use of InSAR in assessing their stability and dynamic precursors to failure.

In 2017, Sentinel-1 SAR backscatter imagery captured the break-up of this arch. The arch was relatively stable on 6 May (Figure 6b) before eventually failing sometime before 12 May (Figure 6c). This failure event occurred relatively early as compared with past events (Kwok, 2005) partly in response to thinner ice conditions and northerly winds (Moore and McNeil, 2018). A sequence of six interferograms with a 6-day temporal baseline covering a timespan of 36 days indicates ice deformation around the failure line up until the failure event (Figure 7). The ice arch features various levels of cm- to m-scale deformation and fractures resulting in fringe discontinuities (Figure 7a) most pronounced near the arch terminus to the south. Near the failure line, there is no sign of a fringe discontinuity up until 12 April (Figure 7a) when the interferogram displays near cross-track parallel fringes indicating compression towards the terminus (Figure 7b). There is a significant contrast in fringe density on either side of the line which may be indicative of a fracture where ice to the west is being compressed more rapidly than the ice close to the coast. The interferogram between 18 – 24 April features widespread coherence loss possibly due to continued compression (Figure 7c). Deformation is less severe from 24 April when fringe density is significantly reduced. However, we notice a fringe discontinuity to the east of the line featuring perpendicular intermediate fringe patterns towards late April (Figure 7d). These patterns develop further into circular patterns often associated with vertical lifts and depressions (Figure 7e) before the whole arch appears to fail through shear motion along this same fault (Figure 7f).

This example demonstrates that it may be possible to detect precursors to break-out events without rigorous inverse model-based interpretation of fringe patterns (e.g., Dammann et al., 2016; Dammann et al., 2018b), which does not easily lend itself to operational workflows. Evaluating the interferograms leading up to the failure of the ice arch, suggests that InSAR has the ability to inform stakeholders of changing stability and ice movement with potential value for an early warning system designed to alert ice users of hazards related to ice movement. Recent and ongoing sea ice decline is leading to an increasing presence of thinner ice in the Canadian Archipelago (Haas and Howell, 2015) and weaker ice due to warmer temperatures (Melling, 2002) may lead to earlier breaching of ice arches. This may in turn result in a larger quantity of advected ice with potentially longer travel paths increasing the severity of such events (Barber et al., 2018; Melling, 2002).

4.3 InSAR as a monitoring tool for landfast ice stability

The method presented in this work has a broad set of potential applications for monitoring including subsea permafrost, biological habitats both beneath and above the ice surface, and ice use by a range of stakeholders. Bottomfast ice is important because it helps aggregating subsea permafrost constraining the location of permafrost-rich shorelines. Utilizing InSAR, it is likely possible to monitor changes in bottomfast ice over time with significant implications for erosion and spring flooding (Dammann et al., 2018c) and the release of methane hydrates (Brothers et al., 2012). With respect to ice users, sea ice navigation near or through landfast

sea ice is presently predominately supported by sea ice charts that map areas occupied by landfast ice, but do not provide information as to the relative stability of the ice. The information provided here would likely be useful in the context of navigation and supporting on-ice operations and could be provided through the InSAR-based approach described here by identifying the following stability-related features:

- 5 1) Low-stability ice that may break off and drift into shipping lanes.
- 2) Grounded ridges that may be problematic for ice navigation, but at the same time may provide added stability for on-ice operations.
- 3) Stable areas to use for equipment staging by coastal community hunters and industry.
- 4) Bottomfast ice for development of ice roads for transportation of heavy loads.

10 In this work, no parameters were changed in the interferometric processing workflow between regions or image pairs emphasizing the possibility of producing ~~these images~~ in a cost-effective manner and by personnel with limited experience with InSAR, similar to semi-automated processing underlying SARVIEWS (<http://sarviews-hazards.alaska.edu>) and Hyp3 (<http://hyp3.asf.alaska.edu>). The method of mapping landfast ice stability is further based on visual interpretation. We have based the analysis strictly on identifying areas of reduced phase response or a strong phase gradient without applying other datasets or advanced interpretation

15 methods such as inverse modeling. Hence, the approach can potentially be adapted by organizations without the need for trained SAR experts. The subjective, manual image interpretation approach **has proven useful in most regions due to the presence of both stabilized and non-stabilized landfast ice**, but is subject to highlighted limitations.

5 Conclusion

In a time of rapidly changing **ice** conditions and continued interest in the Arctic by a range of stakeholders, we stress the need for

20 new assessment strategies to ~~support continued~~ safe and efficient use of sea ice. InSAR is gaining growing attention in the sea ice scientific community and here we demonstrate its value for identifying ~~and mapping newly defined~~ zones of landfast **ice**. We are also highlighting the ~~potentially substantial impact~~ InSAR may have on the development of operational sea ice information products for both long-term strategic planning as well as short-term tactical decisions. Using interferograms generated by a

25 standardized workflow, we show that three stability zones of landfast ice can be identified based on fringe density and continuity, which are indicative of differential ice motion occurring between SAR acquisitions. Along the Beaufort Sea coast of Alaska, we find that the landfast ice regime can be well described with three stability zones: bottomfast ice, where the sea ice is frozen to or resting on the seabed; **stabilized ice, which is floating but anchored by islands or grounded ridges; and non-stabilized ice, which represent floating extensions seaward of any anchoring points. This finding was supported by comparison with the location of stable “nodes” identified through analysis of hundreds of landfast ice edge positions over the period 1996-2008 (Mahoney et al.,**

30 **2014). Not only does this provide some validation of our results, but it demonstrates the ability of InSAR to capture in two snapshots what otherwise requires analysis of data over many years. With that said, the stability zones in the Beaufort Sea and the Russian Arctic appear to be qualitatively different. This makes it challenging to directly adapt the proposed scheme to the East Siberian and Laptev Sea without including additional stability zones. This would allow for a more rigorous definition of landfast sea ice in different regions with implications for operational mapping.**

35 The use of a standardized workflow facilitates large-scale application of this approach, which we demonstrated on a near-pan Arctic scale using 52 Sentinel-1 acquisition pairs during spring 2017. This allowed us to map the same zones of landfast ice in the Beaufort, Chukchi, East Siberian, Laptev, and Kara seas. It also enabled us to estimate and compare the total area covered by each

stability zone in each marginal sea. However, we note that these comparisons are based on the assumption that the landfast ice regimes in all these seas can be well described by the same three stability zones. Although we find evidence that other zones of landfast ice may exist in the Russian Arctic, our results clearly show that not all landfast ice is equally stable. Here, InSAR is potentially able to detect small-scale motions on scales reaching hundreds of km that have previously been overlooked.

5 We further demonstrate the scientific and operational value of InSAR over sea ice through the examination of interferograms of ice arches, which in this context can be considered as an additional stability zones of quasi-landfast ice (e.g., “temporarily stabilized pack ice”). Preliminary analysis of the Nares Strait ice arch in 2017 suggests that interferograms may reveal early-warning signals of an imminent break-up. We also anticipate that inverse modeling of the interferograms of ice arches to estimate the small-scale strain field (Dammann et al., 2018b) may improve our ability to predict their formation. We also show how InSAR can provide
10 valuable information for stakeholders enabling tracking of ice dynamics and stability on seasonal timescales. The ability to provide stability information to stakeholders also opens up for the development of operational guidelines in terms of what stability zones should be prioritized or avoided.

This work builds on previous applications of InSAR to the study of landfast ice (Meyer et al., 2011; Berg et al., 2015; Dammert et al., 1998; Morris et al., 1999; Dammann et al., 2018b) and demonstrates what can be achieved over large areas with a standardized
15 work flow. 2017 was the first year Sentinel-1 covered the Arctic coast with IW images necessary for this analysis. If this coverage continues, there will be considerable opportunity for development beyond what is presented here, including development of automated methods for mapping and classifying landfast ice suitable for incorporation into operational ice charts. Furthermore, through additional analysis of landfast ice and ice arches subject to different forcing conditions, we anticipate improving our understanding of stabilizing and destabilizing mechanisms, thereby allowing improved prediction of formation and break-up. This
20 will not only enhance operational sea ice information available to stakeholders, but also allow us to better understand the response of coastal sea ice to a changing Arctic environment.

Acknowledgements

This work was funded by the Swedish National Space Agency (Dnr. 192/15). Sentinel-1 data are provided free of charge by the European Union Copernicus program. We acknowledge Alaska Satellite Facility for data access and in particular Bill Hauer for
25 valuable data support.

Competing interests

The authors declare that they have no conflict of interest.

References

- ACIA: Impacts of a Warming Arctic, Arctic Climate Impact Assessment, Cambridge University Press, Cambridge, UK, 144 pp., 2004.
- 30 Alexandrov, V. Y., Martin, T., Kolatschek, J., Eicken, H., Kreyscher, M., and Makshtas, A. P.: Sea ice circulation in the Laptev Sea and ice export to the Arctic Ocean: Results from satellite remote sensing and numerical modeling, *Journal of Geophysical Research: Oceans*, 105, 17143-17159, 2000.
- Aporta, C., and Higgs, E.: Satellite culture - Global positioning systems, inuit wayfinding, and the need for a new account of technology, *Curr Anthropol*, 46, 729-753, 10.1086/432651, 2005.
- 35 Are, F., and Reimnitz, E.: An overview of the Lena River Delta setting: geology, tectonics, geomorphology, and hydrology, *Journal of Coastal Research*, 16, 1083-1093, 2000.
- Bailey, W.: Oceanographic features of the Canadian Archipelago, *Journal of the Fisheries Board of Canada*, 14, 731-769, 1957.
- Bamler, R., and Hartl, P.: Synthetic aperture radar interferometry, *Inverse problems*, 14, R1, 1998.

- Barber, D., Babb, D., Ehn, J., Chan, W., Matthes, L., Dalman, L., Campbell, Y., Harasyn, M., Firoozy, N., and Theriault, N.: Increasing mobility of high Arctic sea ice increases marine hazards off the east coast of Newfoundland, *Geophys Res Lett*, 45, 2370-2379, 2018.
- Bell, T., Briggs, R., Bachmayer, R., and Li, S.: Augmenting Inuit knowledge for safe sea-ice travel—The SmartICE information system, 2014 Oceans'14 St. John's, Newfoundland, 2014, 1-9, 2014.
- 5 Berg, A., Dammert, P., and Eriksson, L. E. B.: X-Band Interferometric SAR Observations of Baltic Fast Ice, *IEEE Transactions on Geoscience and Remote Sensing*, 53, 1248-1256, 10.1109/TGRS.2014.2336752, 2015.
- Brothers, L. L., Hart, P. E., and Ruppel, C. D.: Minimum distribution of subsea ice-bearing permafrost on the US Beaufort Sea continental shelf, *Geophys Res Lett*, 39, 10.1029/2012GL052222 2012.
- 10 Comiso, J. C., and Hall, D. K.: Climate trends in the Arctic as observed from space, *Wiley Interdisciplinary Reviews: Climate Change*, 5, 389-409, 10.1002/wcc.277, 2014.
- Dammann, D. O., Eicken, H., Meyer, F., and Mahoney, A.: Assessing small-scale deformation and stability of landfast sea ice on seasonal timescales through L-band SAR interferometry and inverse modeling, *Remote Sens Environ*, 187, 492-504, 10.1016/j.rse.2016.10.032, 2016.
- Dammann, D. O.: Arctic sea ice trafficability - new strategies for a changing icescape, Ph.D. thesis, Department of Geosciences, University of Alaska Fairbanks, Fairbanks, Alaska, USA, 217 pp., 2017.
- 15 Dammann, D. O., Eicken, H., Sait, E., Mahoney, A., Meyer, F., and George, J. C.: Traversing sea ice - linking surface roughness and ice trafficability through SAR polarimetry and interferometry *IEEE Journal of Selected Topics in Applied Earth Observations and Remote Sensing*, 11, 416-433, 10.1109/JSTARS.2017.2764961, 2017.
- Dammann, D. O., Eicken, H., Mahoney, A., Meyer, F., and Betcher, S.: Assessing sea ice trafficability in a changing Arctic, *Arctic*, 71, 59-75, 10.14430/arctic4701, 2018a.
- 20 Dammann, D. O., Eicken, H., Mahoney, A., Meyer, F., Freymueller, J., and Kaufman, A. M.: Evaluating landfast sea ice stress and fracture in support of operations on sea ice using SAR interferometry, *Cold Reg Sci Technol*, 10.1016/j.coldregions.2018.02.001, 2018b.
- Dammann, D. O., Eriksson, L. E. B., Mahoney, A., Stevens, C. W., Van der Sanden, J., Eicken, H., Meyer, F., and Tweedie, C.: Mapping Arctic bottomfast sea ice using SAR interferometry, *Remote Sensing*, 10(5), 720, 10.3390/rs10050720, 2018c.
- Dammert, P. B. G., Lepparanta, M., and Askne, J.: SAR interferometry over Baltic Sea ice, *Int J Remote Sens*, 19, 3019-3037, 25 10.1080/014311698214163, 1998.
- Dierking, W., Lang, O., and Busche, T.: Sea ice local surface topography from single-pass satellite InSAR measurements: a feasibility study, *The Cryosphere*, 11, 1967, 10.5194/tc-11-1967-2017, 2017.
- Druckenmiller, M. L.: Alaska shorefast ice: interfacing geophysics with local sea ice knowledge and use, Ph.D. thesis, University of Alaska Fairbanks, Fairbanks, Alaska, 210 pp., 2011.
- 30 Druckenmiller, M. L., Eicken, H., George, J. C., and Brower, L.: Trails to the whale: reflections of change and choice on an Inupiat icescape at Barrow, Alaska, *Polar Geography*, 36, 5-29, 10.1080/1088937X.2012.724459, 2013.
- Eguíluz, V. M., Fernández-Gracia, J., Irigoien, X., and Duarte, C. M.: A quantitative assessment of Arctic shipping in 2010–2014, *Scientific reports*, 6, 30682, 2016.
- 35 Eicken, H., Dmitrenko, I., Tyshko, K., Darovskikh, A., Dierking, W., Blahak, U., Groves, J., and Kassens, H.: Zonation of the Laptev Sea landfast ice cover and its importance in a frozen estuary, *Global and planetary change*, 48, 55-83, 2005.
- Eicken, H., Lovcraft, A. L., and Druckenmiller, M. L.: Sea-Ice System Services: A Framework to Help Identify and Meet Information Needs Relevant for Arctic Observing Networks, *Arctic*, 62, 119-136, 10.14430/arctic126, 2009.
- Eicken, H., Jones, J., Meyer, F., Mahoney, A., Druckenmiller, M. L., Rohith, M., and Kambhamettu, C.: Environmental security in Arctic ice-covered seas: from strategy to tactics of hazard identification and emergency response, *Mar Technol Soc J*, 45, 37-48, 40 doi.org/10.4031/MTSJ.45.3.1, 2011.
- Eicken, H., and Mahoney, A. R.: Sea Ice: Hazards, Risks, and Implications for Disasters, in: *Coastal and Marine Hazards, Risks, and Disasters*, edited by: Ellis, J. T., Sherman, D. J., and Shroder, J. F., Elsevier Inc., Amsterdam, Netherlands, 381-399, 2015.
- Ellis, B., and Brigham, L.: Arctic marine shipping assessment, Akureyri, Island, 2009.
- 45 Ferretti, A., Monti-Guarnieri, A., Prati, C., Rocca, F., and Massonet, D.: *InSAR Principles-Guidelines for SAR Interferometry Processing and Interpretation*, ESA Publications, TM-19, 2007.
- Fienuup-Riordan, A., and Rearden, A.: The ice is always changing: Yup'ik understandings of sea ice, past and present, in: *SIKU: knowing Our Ice: Documenting Inuit Sea Ice knowledge and Use*, edited by: Krupnik, I., Aporta, C., Gearheard, S., Laidler, G., and Holm, L. K., Springer, New York, 295-320, 2010.
- 50 Ford, J. D., Pearce, T., Gilligan, J., Smit, B., and Oakes, J.: Climate change and hazards associated with ice use in northern Canada, *Arctic, Antarctic, and Alpine Research*, 40, 647-659, 10.1657/1523-0430(07-040)[FORD]2.0.CO;2, 2008.
- Giles, A. B., Massom, R. A., and Lytle, V. I.: Fast-ice distribution in East Antarctica during 1997 and 1999 determined using RADARSAT data, *Journal of Geophysical Research: Oceans*, 113, 10.1029/2007JC004139, 2008.
- Goldstein, R. M., and Werner, C. L.: Radar interferogram filtering for geophysical applications, *Geophys Res Lett*, 25, 4035-4038, 1998.
- Haas, C., and Howell, S. E.: Ice thickness in the Northwest Passage, *Geophys Res Lett*, 42, 7673-7680, 2015.
- 55 Hibler, W., Hutchings, J., and Ip, C.: Sea-ice arching and multiple flow states of Arctic pack ice, *Annals of Glaciology*, 44, 339-344, 2006.
- Hirose, T., Kapfer, M., Bennett, J., Cott, P., Manson, G., and Solomon, S.: Bottomfast Ice Mapping and the Measurement of Ice Thickness on Tundra Lakes Using C-Band Synthetic Aperture Radar Remote Sensing, *JAWRA Journal of the American Water Resources Association*, 44, 285-292, 2008.
- Howell, S. E., Wohlleben, T., Dabboor, M., Derksen, C., Komarov, A., and Pizzolato, L.: Recent changes in the exchange of sea ice between the 60 Arctic Ocean and the Canadian Arctic Archipelago, *Journal of Geophysical Research: Oceans*, 118, 3595-3607, 2013.
- Hui, F., Zhao, T., Li, X., Shokr, M., Heil, P., Zhao, J., Zhang, L., and Cheng, X.: Satellite-Based Sea Ice Navigation for Prydz Bay, East Antarctica, *Remote Sensing*, 9, 518, 2017.
- Johannessen, O. M., Alexandrov, V., Frolov, I. Y., Sandven, S., Pettersson, L. H., Bobylev, L. P., Kloster, K., Smirnov, V. G., Mironov, Y. U., and Babich, N. G.: *Remote sensing of sea ice in the Northern Sea Route: studies and applications*, Springer Science & Business Media, Chichester, 65 United Kingdom, 2006.
- Jones, J. M., Eicken, H., Mahoney, A. R., Rohith, M. V., C., K., Y., F., I., O. K., and George, J. C.: Landfast sea ice breakouts: Stabilizing ice features, oceanic and atmospheric forcing at Barrow, Alaska, *Continental Shelf Research*, 126, 10.1016/j.csr.2016.07.015, 2016.

- Krupnik, I., Aporta, C., Gearheard, S., Laidler, G. J., and Holm, L. K.: SIKU: knowing our ice, Springer, New York, 2010.
- Kwok, R.: Variability of Nares Strait ice flux, *Geophys Res Lett*, 32, 2005.
- Kwok, R.: Exchange of sea ice between the Arctic Ocean and the Canadian Arctic Archipelago, *Geophys Res Lett*, 33, 2006.
- Kwok, R., Toudal Pedersen, L., Gudmandsen, P., and Pang, S.: Large sea ice outflow into the Nares Strait in 2007, *Geophys Res Lett*, 37, L03502, 10.1029/2009GL041872, 2010.
- 5 Li, S., Shapiro, L., McNutt, L., and Feffers, A.: Application of Satellite Radar Interferometry to the Detection of Sea Ice Deformation, *Journal of the Remote Sensing Society of Japan*, 16, 67-77, 1996.
- Lovecraft, A. L., and Eicken, H.: North by 2020: perspectives on Alaska's changing social-ecological systems, University of Alaska Press, Fairbanks, Alaska, 2011.
- 10 Mahoney, A., Eicken, H., Graves, A., Shapiro, L., and Cotter, P.: Landfast sea ice extent and variability in the Alaskan Arctic derived from SAR imagery, *Proceedings of the International Geoscience and Remote Sensing Symposium*, Anchorage, AK, 2004, 2146-2149, 2004.
- Mahoney, A., Eicken, H., Gaylord, A. G., and Shapiro, L.: Alaska landfast sea ice: Links with bathymetry and atmospheric circulation, *Journal of Geophysical Research: Oceans*, 112, 10.1029/2006JC003559, 2007a.
- 15 Mahoney, A., Eicken, H., and Shapiro, L.: How fast is landfast sea ice? A study of the attachment and detachment of nearshore ice at Barrow, Alaska, *Cold Reg Sci Technol*, 47, 233-255, 10.1016/J.Coldregions.2006.09.005, 2007b.
- Mahoney, A., Eicken, H., Gaylord, A. G., and Gens, R.: Landfast sea ice extent in the Chukchi and Beaufort Seas: The annual cycle and decadal variability, *Cold Reg Sci Technol*, 103, 41-56, 10.1016/J.Coldregions.2014.03.003, 2014.
- Marbouti, M., Praks, J., Antropov, O., Rinne, E., and Leppäranta, M.: A Study of Landfast Ice with Sentinel-1 Repeat-Pass Interferometry over the Baltic Sea, *Remote Sensing*, 9, 833, 10.3390/rs9080833, 2017.
- 20 Meier, W. N., Hovelsrud, G. K., Oort, B. E., Key, J. R., Kovacs, K. M., Michel, C., Haas, C., Granskog, M. A., Gerland, S., and Perovich, D. K.: Arctic sea ice in transformation: A review of recent observed changes and impacts on biology and human activity, *Reviews of Geophysics*, 52, 185-217, 2014.
- Melling, H.: Sea ice of the northern Canadian Arctic Archipelago, *Journal of Geophysical Research: Oceans*, 107, 2002.
- Meyer, F. J., Mahoney, A. R., Eicken, H., Denny, C. L., Druckenmiller, H. C., and Hendricks, S.: Mapping arctic landfast ice extent using L-band synthetic aperture radar interferometry, *Remote Sens Environ*, 115, 3029-3043, 10.1016/J.Rse.2011.06.006, 2011.
- 25 Meyer, F. J., McAlpin, D., Gong, W., Ajadi, O., Arko, S., Webley, P., and Dehn, J.: Integrating SAR and derived products into operational volcano monitoring and decision support systems, *ISPRS Journal of Photogrammetry and Remote Sensing*, 100, 106-117, 2015.
- Moore, G., and McNeil, K.: The early collapse of the 2017 Lincoln Sea ice arch in response to anomalous sea ice and wind forcing, *Geophys Res Lett*, 2018.
- 30 Morris, K., Li, S., and Jeffries, M.: Meso- and microscale sea-ice motion in the East Siberian Sea as determined from ERS-I SAR data, *Journal of Glaciology*, 45, 370-383, 1999.
- Muckenhuber, S., and Sandven, S.: Open-source sea ice drift algorithm for Sentinel-1 SAR imagery using a combination of feature tracking and pattern matching, *The Cryosphere*, 11, 1835, 2017.
- Onstott, R. G.: SAR and scatterometer signatures of sea ice, *Microwave remote sensing of sea ice*, 73-104, 1992.
- 35 Orviku, K., Jaagus, J., and Tõnisson, H.: Sea ice shaping the shores, *Journal of Coastal Research*, 681, 2011.
- Potter, R., Walden, J., and Haspel, R.: Design and construction of sea ice roads in the Alaskan Beaufort Sea, *Offshore Technology Conference*, Houston, Texas, 1981.
- Reimnitz, E., Dethleff, D., and Nürnberg, D.: Contrasts in Arctic shelf sea-ice regimes and some implications: Beaufort Sea versus Laptev Sea, *Marine Geology*, 119, 215-225, 1994.
- 40 Scharroo, R., and Visser, P.: Precise orbit determination and gravity field improvement, *Journal of Geophysical Research*, 103, 8113-8127, 1998.
- Screen, J. A., and Simmonds, I.: The central role of diminishing sea ice in recent Arctic temperature amplification, *Nature*, 464, 1334-1337, 2010.
- Selyuzhenok, V., Krumpen, T., Mahoney, A., Janout, M., and Gerdes, R.: Seasonal and interannual variability of fast ice extent in the southeastern Laptev Sea between 1999 and 2013, *Journal of Geophysical Research: Oceans*, 120, 7791-7806, 10.1002/2015JC011135, 2015.
- 45 Selyuzhenok, V., Mahoney, A., Krumpen, T., Castellani, G., and Gerdes, R.: Mechanisms of fast-ice development in the south-eastern Laptev Sea: a case study for winter of 2007/08 and 2009/10, *Polar Research*, 36, 1411-1440, 2017.
- Smith, T. G.: Polar bear predation of ringed and bearded seals in the land-fast sea ice habitat, *Canadian Journal of Zoology*, 58, 2201-2209, 1980.
- Solomon, S. M., Taylor, A. E., and Stevens, C. W.: Nearshore ground temperatures, seasonal ice bonding, and permafrost formation within the bottom-fast ice zone, Mackenzie Delta, NWT, *Proceedings of the Ninth International Conference on Permafrost*, University of Alaska Fairbanks, Fairbanks, Alaska, 2008, 1675-1680, 2008.
- 50 Stephenson, S. R., Smith, L. C., and Agnew, J. A.: Divergent long-term trajectories of human access to the Arctic, *Nat Clim Change*, 1, 156-160, 10.1038/Nclimate1120, 2011.
- Stevens, C. W., Moorman, B. J., and Solomon, S. M.: Detection of frozen and unfrozen interfaces with ground penetrating radar in the nearshore zone of the Mackenzie Delta, Canada, *Proceedings of the Ninth International Conference on Permafrost*, University of Alaska Fairbanks, Fairbanks, Alaska, 2008, 1711-1716, 2008.
- 55 Stevens, C. W., Moorman, B. J., and Solomon, S. M.: Interannual changes in seasonal ground freezing and near-surface heat flow beneath bottom-fast ice in the near-shore zone, Mackenzie Delta, NWT, Canada, *Permafrost and Periglacial Processes*, 21, 256-270, 2010.
- Stevens, C. W.: Controls on Seasonal Ground Freezing and Permafrost in the Near-shore Zone of the Mackenzie Delta, NWT, Canada, University of Calgary, 2011.
- Stroeve, J. C., Serreze, M. C., Holland, M. M., Kay, J. E., Malanik, J., and Barrett, A. P.: The Arctic's rapidly shrinking sea ice cover: a research synthesis, *Climatic Change*, 110, 1005-1027, 10.1007/S10584-011-0101-1, 2012.
- 60 Thomas, D. N.: Sea ice, John Wiley & Sons, Chichester, United Kingdom, 2017.
- Tibbles, M., Falke, J. A., Mahoney, A. R., Robards, M. D., and Seitz, A. C.: An In SAR habitat suitability model to identify overwinter conditions for coregonine whitefishes in Arctic lagoons, *Transactions of the American Fisheries Society*, In press.
- Vincent, F., Raucoules, D., Degroev, T., Edwards, G., and Abolfazl Mostafavi, M.: Detection of river/sea ice deformation using satellite interferometry: limits and potential, *Int J Remote Sens*, 25, 3555-3571, 2004.
- 65 Werner, C., Wegmüller, U., Strozz, T., and Wiesmann, A.: Gamma SAR and interferometric processing software, *Proceedings of the ERS-ENVISAT symposium*, Gothenburg, Sweden, 2000, 1620

Wessel, P., and Smith, W. H.: A global, self-consistent, hierarchical, high-resolution shoreline database, *Journal of Geophysical Research: Solid Earth*, 101, 8741-8743, 1996.

Wilson, K. J., Falkingham, J., Melling, H., and De Abreu, R.: Shipping in the Canadian Arctic: other possible climate change scenarios, *Proceedings of the International Geoscience and Remote Sensing Symposium*, Anchorage, AK, 2004, 1853-1856, 2004.

- 5 Yu, Y., Stern, H., Fowler, C., Fetterer, F., and Maslanik, J.: Interannual Variability of Arctic Landfast Ice between 1976 and 2007, *J Climate*, 27, 227-243, 10.1175/JCLI-D-13-00178.1, 2014.

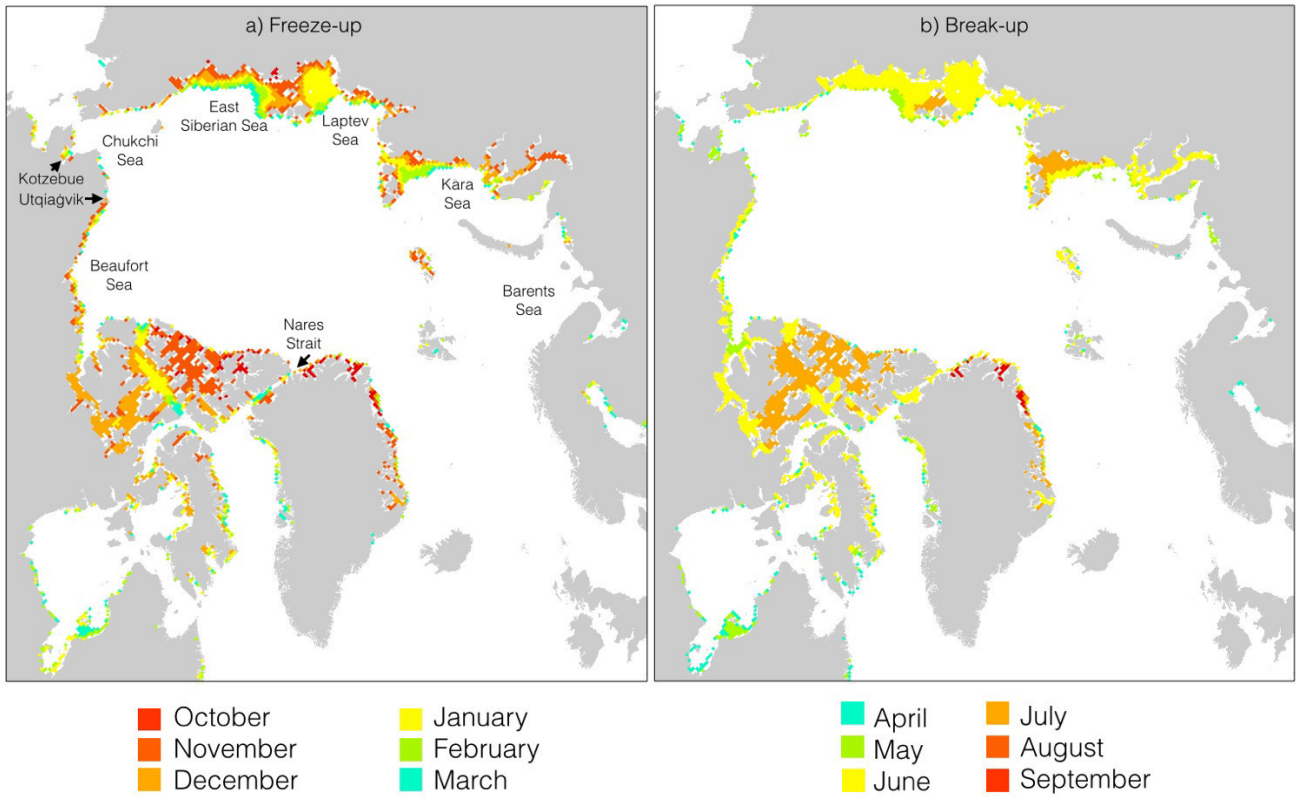


Figure 1: (a) Oct - Mar (Freeze-up) and (b) Apr - Sep (break-up) monthly mean landfast sea ice extent (1976 - 2007) derived from sea ice charts based on optical instruments and SAR. The data for this figure was obtained from the National Snow and Ice Data Center (Yu et al., 2014).

5

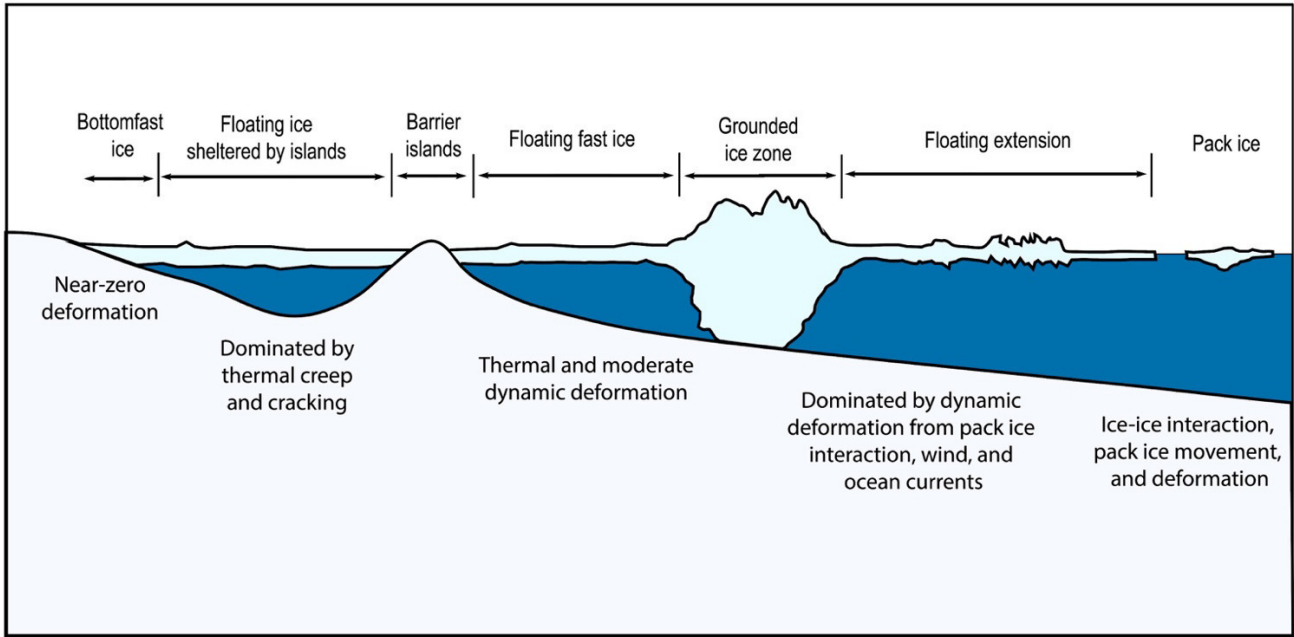
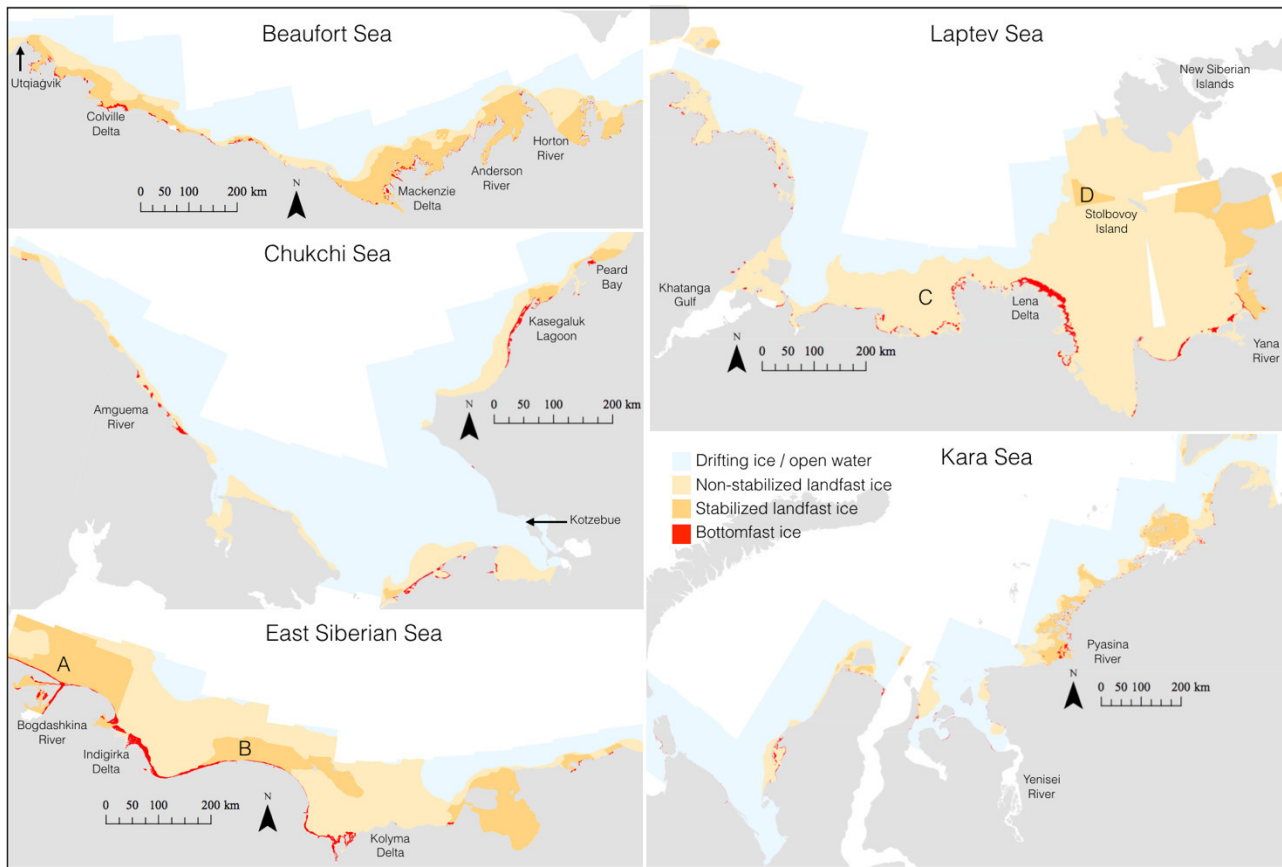


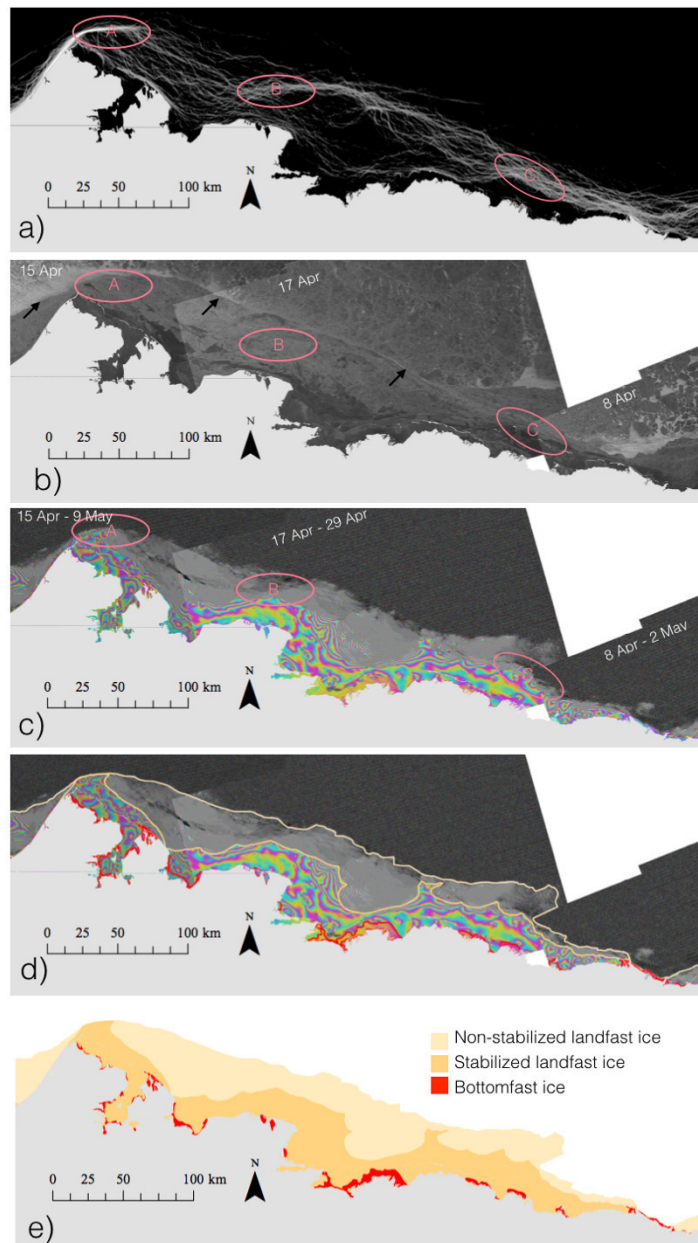
Figure 2: Conceptual scheme of landfast sea ice where different regimes possess different levels of stability.



5 **Figure 3: 52 Sentinel-1 interferograms derived from image pairs acquired between February and May, 2017. Numbers on images represent date ranges where the colors blue, green, yellow, and red signify the months of February-May respectively.**



5 **Figure 4: InSAR-derived map of non-stabilized and stabilized landfast ice and bottomfast ice from 52 Sentinel-1 image pairs acquired predominately between March and May, 2017. Letters A-D mark areas discussed in the text. Land is masked out in grey. Due to minor inaccuracies in the landmask, the occurrence of bottomfast ice can appear sporadic.**



5 Figure 5: (a) Landfast ice edge occurrence mapped for the period 1996–2008 over the Alaska Beaufort Sea (Mahoney et al. 2014). Light red circles correspond to areas of frequent landfast ice edge formation referred to as “nodes”, (b) and (c) Sentinel-1 backscatter images and interferograms of landfast ice between mid-April and mid-May 2017, (d) map of landfast ice, grounded landfast ice, and bottomfast ice superimposed on the interferograms, and (e) different landfast ice regimes derived from the interferograms.

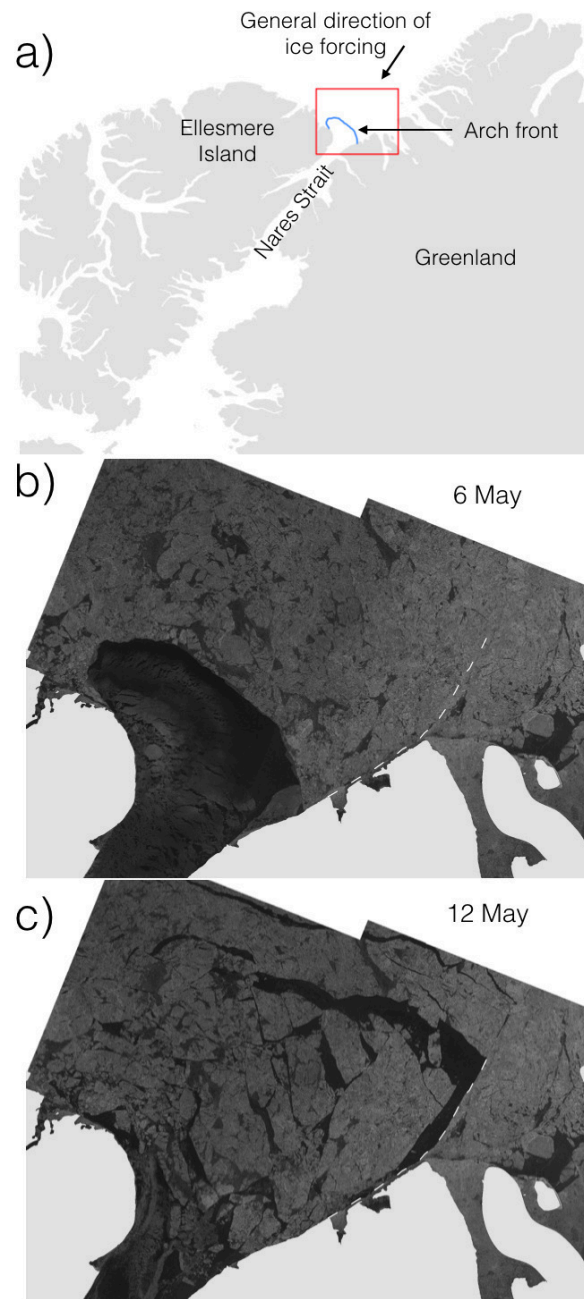


Figure 6: (a) overview of Nares Strait and location, location of Sentinel-1 imagery (red rectangle), and delineation of the arch (blue line) as obtained from (b). Backscatter images over the 2017 ice arch before (b) and after (c) failure. The line of failure is identified in Figure 6b and marked as a dashed line in both (b) and (c). Land is masked out in light gray.

5

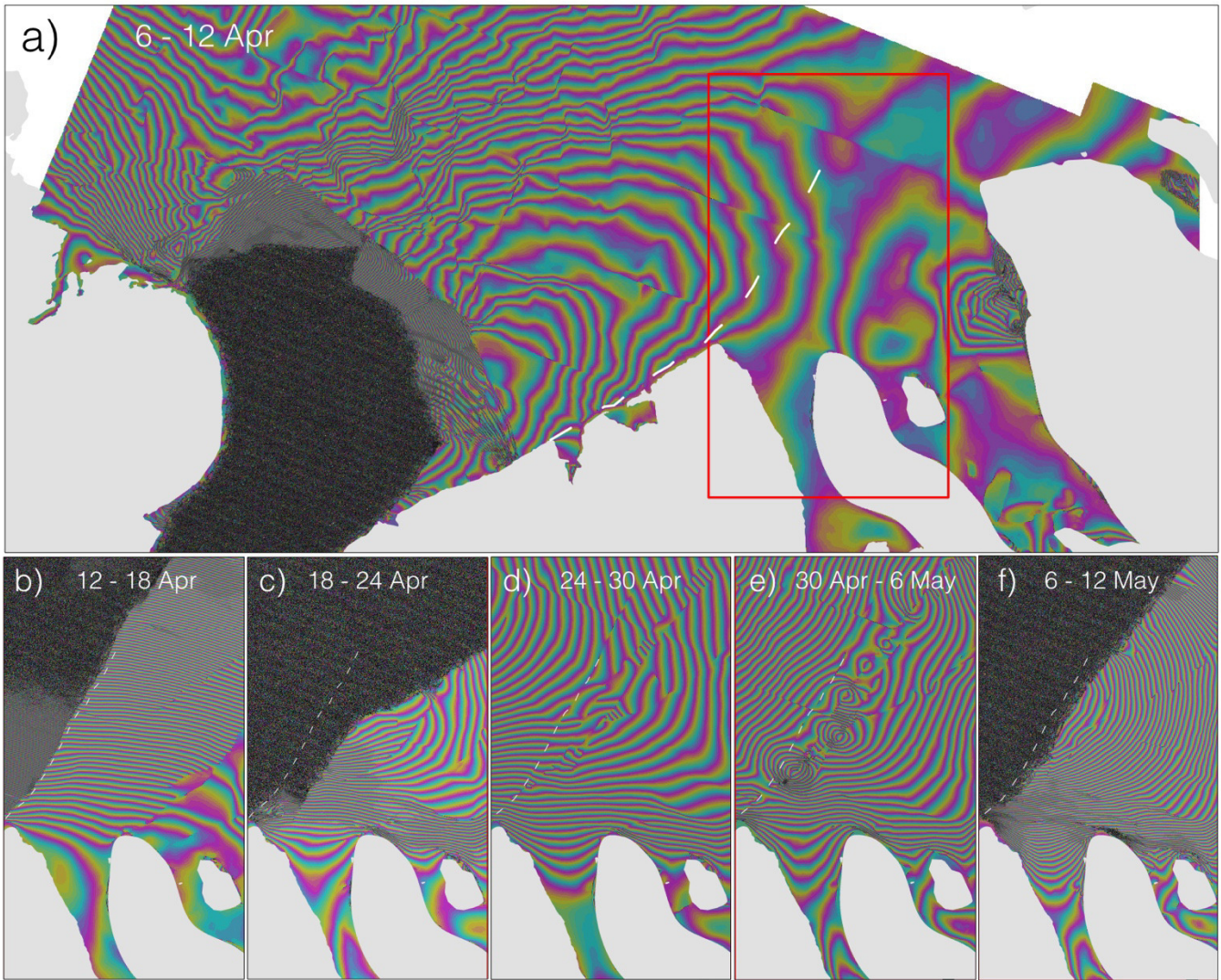


Figure 7: Interferogram over the Nares Strait ice arch in 2017 covering the time period 6 - 12 Apr. (a). Smaller panels show consecutive interferograms within the box for 12 - 18 Apr (b), 18 - 24 Apr (c), 24 - 30 Apr (d), 30 Apr - 6 May (e), and 6 - 12 May (f). The dashed line represents the line separating the fast and moving ice in Figure 6b. Land is masked out in light gray.

5

Table 1: Landfast sea ice stability regimes and assigned stability zones identified using InSAR and typical deformation rates

	Landfast ice regime	Stability	Stability zone	Identified by	Deformation rate (cm/km/month)
1	Bottomfast sea ice (i.e., ice frozen to or in broad contact with the sea floor)	Completely stable. Ice is frozen to or resting on the sea floor restricting lateral motion. Vertical tide jacking may occur and subsides as the ice thickens.	Bottomfast	No identifiable phase difference from the adjacent land	0
2	Floating ice sheltered in lagoons or fjords	High stability. Ice is largely enclosed by land and is sheltered from more dynamic ice. Deformation is dominated by cm- to dm-scale thermal creep and fracture.	Stabilized	Poorly defined, widely spaced fringes or abruptly reduced fringe spacing compared to offshore ice	~0.1 – ~1
3	Floating ice sheltered by grounded ridges or islands	Moderate stability. Ice is supported by point features largely inhibiting break out events. In addition to thermal creep, internal stress from more dynamic ice can propagate in between pinning points resulting in dm- to m-scale non-elastic deformation.			
4	Floating ice extensions	Low stability. Dominated by m-scale deformation from ice, wind, and ocean forcing. Persistent inelastic deformation can lead to accumulated strain on the order of tens of meters on time-scales exceeding several weeks. The ice may remain attached (Mahoney et al., 2004) or can break-off from the stabilized ice.	Non-stabilized		< ~100

Table 2: Approximate area coverage of landfast ice regimes (in thousand km²).

Area	Bottomfast ice	Stabilized	Non- stabilized	Total area of landfast ice	Non-stabilized / stabilized
Beaufort Sea	2.5	35	30	65	0.86
Chukchi Sea	1.8	0.95	27	29	28
East Siberian Sea	5.1	40	81	126	2.0
Laptev Sea	4.1	33	164	201	5.0
Kara Sea	2.5	16	38	56	2.4

The bottomfast zone is constrained between its outer extent interpreted from the phase and the coast as interpreted from the backscatter scenes. The stabilized zone is constrained between its outer extent as interpreted from the phase and the bottomfast ice or the landmask (Wessel and Smith, 1996). The non-stabilized ice is constrained between the outer extent of significant coherence and the bottomfast ice, stabilized ice, or the landmask.